

BME0005

Numerical Simulation of Alveolar Bone Regeneration and Angiogenesis - Trabecular Bone Formation -

Y. Fukuda¹, Katsuya Nagayama^{1*} and Masato Matsuo²

¹ Kyushu Institute of Technology, 680-4 Kawazu, Iizuka, Fukuoka, 820-8502, Japan

² Kanagawa Dental University, 82 Inaokacho, Yokosuka, Kanagawa, 238-8580, Japan

* Corresponding Author: nagayama@mse.kyutech.ac.jp, Tel & Fax 81-948-29-7778

Abstract

Alveolar bone is the substance that supports teeth. Regeneration of alveolar bone after tooth extraction is known to be adaptive and requires Ca^{2+} , which is secreted from local blood vessels. Thus, there is a strong relation between alveolar bone regeneration and both angiogenesis and Ca^{2+} secreted from blood vessels. In addition, bone formation is affected by the mechanical force around it and by shape remodeling by osteoblasts and osteoclasts. Therefore, in this study, an angiogenesis model, a Ca^{2+} transport model, a stress analysis model, and a reaction-diffusion model are constructed and calculated at the same time as a coupled analysis model of trabecular bone formation. Thus, our final bone regeneration model is constructed using the above factors and compared with data and images of the actual phenomena.

Keywords: Numerical Simulation, Bone Formation, Angiogenesis, Vascular Regression, Trabecular Bone

1. Introduction

First, in clinical regenerative medicine, blood circulation is essential for nutrient supply. Recent studies have focused on how to attract blood vessels for regeneration. Further, platelet-rich plasma (PRP)[1-4], which promotes wound healing, has attracted attention in this regard; however its effects cannot be predicted yet. In this study, we built a simulator to predict the interaction with angiogenesis in alveolar bone regeneration with the aim of applying the results in the field of clinical regenerative medicine.

Second, the bone has been found to have self-adjusting capabilities to functionally adapt to relative changes in the mechanical environment. Bones as well as other biological tissue always undergo dynamic remodeling to maintain homeostasis. However, many aspects of the bone formation mechanism remain unclear. Therefore, we first built a dynamic factor model. Then, we reproduced the functional adaptation characteristics of bone with mechanical computer stimulation. The aim of the study was to contribute toward understanding the mechanism of bone formation.

2. Analysis Object

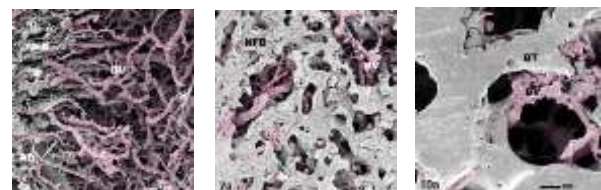
Figs. 1 and 2 were obtained from bone regeneration experiments [1] in which mandibular premolars were extracted from beagle dogs. The gingival flap was then sutured. Microvascular resin injections were performed after 14, 30, and 90 days. From the 14th day to the 30th day, angiogenesis occurred in order to provide a lot of nutrition, and immature bone formed. After the 30th day, the bone became stronger and was optimized structurally. Then trabecular bone formed. When the trabecular formation is advanced, nutrition transport is saturated. So, blood vessels with small diameters that are no longer necessary bury themselves in the bone, or

regress. We reproduced the phenomena seen in these experimental images with our analysis model.

In this study, a mathematical model was also constructed for qualitative and quantitative comparison.



Fig. 1 Macroscale Images of Alveolar Bone after Tooth Extraction (8 mm × 4 mm)



(a) Day 14 (b) Day 30 (c) Day 90

Fig. 2 Microscale Images of Alveolar Bone after Tooth Extraction (1 mm × 1 mm)

3. Methods

Analyses in this study were performed using a particle model [3]. The positional relationship is not constrained between the particles in this model, thereby allowing complex analysis of the data.

Regeneration of alveolar bone is affected by many factors such as angiogenesis, Ca^{2+} secreted from blood vessels, and the surrounding mechanical environment. The models for each factor influencing bone formation are described below.

BME0005

3.1 Angiogenesis Model

Bone regeneration is considerably affected by angiogenesis because the blood vessels supply the nutrients necessary for bone formation[1-5]. Angiogenesis is the formation of new blood vessels by extending and repetitively migrating and branching vascular endothelial cells. In Fig. 1, the interior of the alveolar bone shows blood clots at the center due to bleeding following tooth extraction; blood vessels extend toward this section. Concurrent with angiogenesis, Ca^{2+} is secreted from the blood vessels. The Ca^{2+} in the area thus surrounding the blood vessels is used for bone regeneration. Because blood vessels extend toward the center of the tooth, as shown in Fig. 1, a higher incentive value of angiogenesis is found closer to the center compared with over the entire area in the initial state.

The growth processes of blood vessels in this model are as follows. First, the surrounding blood vessels are examined. Next, the particle with the highest incentive value is selected in the direction of elongation (0–30°) or branching (60–80°). Then, blood vessels extend toward the selected particle with the highest incentive value. In addition, angiogenesis is adjusted to rule out duplicate or converging vessels by monitoring the density of particles. Because the growing speed of blood vessels varies with PRP [1], its concentration was set as a variable in the analysis.

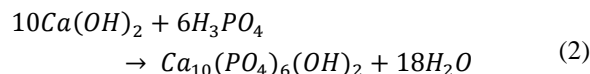
3.2 Ca^{2+} Transport Model

As described in section 3.1, Ca^{2+} is secreted from newly formed blood vessels and diffused throughout the entire area. We assumed that calcium is secreted steadily. The equation used to model Ca^{2+} transport is

$$d_A \nabla^2 A = \frac{1}{\beta} \frac{\partial \rho}{\partial t}, \quad (1)$$

where A is the Ca^{2+} concentration, t is the time, ρ is the bone density, d_A is the diffusion coefficient, and β is the mass ratio of Ca^{2+} and bone. The left-hand side represents the diffusion of Ca^{2+} . The right side represents Ca^{2+} consumption, and it calculates the amount of Ca^{2+} that is consumed during bone formation.

Ca^{2+} that diffuses into the area changes to hydroxyapatite, which is the main component of bone, and is calculated as



Under normal conditions, the Ca^{2+} concentration of blood is between 8.8 and 10.0 mg/dl. Therefore, in this analysis, blood Ca^{2+} concentration is set as a boundary condition with a constant value of 10.0 mg/dl. The boundary condition for the analysis region is set as free because Ca^{2+} flows to the exterior.

3.3 Stress Analysis Model

Bone structure adapts to the load environment because suitable mechanical stimulus encourages bone

growth. It has been reported that strain energy effects bone growth with respect to strength or bone density [9-11].

Alveolar bone is maintained due to stimulation caused by the force of biting. Therefore, in the analysis of alveolar bone regeneration, the distribution of stress on the bone is important. Therefore, in this study, a stress analysis of the newly formed bone is performed using the balance equation of force, which is given by

$$\frac{\partial \tau_{xy}}{\partial x} + \frac{\partial \sigma_y}{\partial y} + \frac{\partial \tau_{yz}}{\partial z} = 0, \quad (3)$$

where σ is the normal stress and τ is the shear stress. Incidentally, this analysis assumes an isotropic elastic incompressible medium for simplicity.

The process of stress analysis is as follows. First, forced displacements were subjected to the boundary particle, and the other boundary particles were set as boundary free. The forced displacements decrease with the passage of time because the bone becomes hard. Second, the strain ε is derived from each part of the displacement, which is transmitted to the entire area by an external force. Next, the strain energy U distribution is calculated using the following equation:

$$U = \frac{1}{2} E \varepsilon^2, \quad (4)$$

where E is Young's modulus. Young's modulus is derived from the relation (Carter and Hayes, 1977) [9-11]:

$$E = c\rho^3 \quad (5)$$

The Young's modulus when bone density is 0.5 mg/mm³ is assumed to be 480 MPa. Poisson's ratio is assumed to be 0.23 [3].

3.4 Reaction-diffusion System Model

In order to produce the bone structure in our analysis, a reaction-diffusion model was introduced. It is essential for forming a bone scaffold that is not influenced by small differences in the initial field. The reaction-diffusion model is based on the transmission of mechanical stimulation between bone cells [6-8]. Remodeling phenomena, which occur due to mechanical stimulation, are influenced not only by temporal regulation but also spatial regulation, which depends on the distance and placement between cells. That is, it is necessary to consider not only the temporal regulation but also the spatial regulation, which can be achieved by monitoring, for example, biochemical processes on the microscopic cellular level, such as intercellular communication and signal molecule diffusion, which are dependent on distance and arrangement. Therefore, in this study, in order to reproduce the trabecular structure that satisfies the shape optimization criteria, we assumed that these processes disperse the mechanical burden for our model of diffusion (transfer) of intercellular communication and signal molecules at the microscopic cellular level. Therefore, the equation of

BME0005

bone formation using bone density ρ is assumed to be as follows:

$$\frac{d\rho}{dt} = d_\rho \nabla^2 \rho \quad (0.0 \leq \rho \leq 0.5) , \quad (6)$$

where d_ρ is the diffusion coefficient. The boundary conditions of the diffusion of bone density were set as periodic boundary conditions. In this study, as shown in Section 3.3, mechanical stimulus is given as a strain energy density U . The strain energy density U is a function of bone density.

3.5 Bone Formation Model

Huiskes and coworkers designed a model that relates to bone formation using strain energy U and Young's modulus E : [9]

$$\frac{dE}{dt} = C(U - U_h) , \quad (7)$$

where t is time, C is a constant, and U_h is the homeostatic strain energy. [5]

In this study, it is assumed that the factors for bone regeneration are independent of each other. Therefore, bone formation is defined as the growth of bone density and is modeled using the following equation:

$$\frac{\partial \rho}{\partial t} = C_A (A) + C_U (U^{\frac{1}{3}} - U_h^{\frac{1}{3}}) + d_\rho \nabla^2 \rho \quad (8) \quad (0.0 \leq \rho \leq 0.5) ,$$

where A is the Ca^{2+} concentration, U is strain energy, d_ρ is the diffusion coefficient, C_A and C_U are constants, A_h is assumed as the homeostatic Ca^{2+} concentration of 3.0 mg/dl of saliva, and U_h is the homeostatic strain energy, which is a value that differs with each patient. On the right side of Equation (8), the first term shows that the denser the bone is, the higher the rate of bone growth is. If the Ca^{2+} concentration is smaller than the homeostatic value A_h , bone dissolves. The second term on the right-hand side of Equation (8) indicates that strain energy becomes a burden on local bone and promotes bone growth. The third term on the right-hand side of Equation (8) indicates the effects of reaction and diffusion on bone formation.

3.6 Modeling of Vascular Regression

When the bone is in a state of underdevelopment, angiogenesis is activated in order to promote growth and to actively transport nutrition to the bone. When the time has elapsed and the bone has grown some extent, nutrition transport is saturated. Then blood vessels, except for thick major one, regress into areas well-saturated with nutrients. Vascular regression arises after blood vessels have spread throughout the region.

In this model, we first detect the average bone density of the peripheral blood vessels. If the average bone density is greater than the threshold, blood vessels regress from the narrow end of the tip. We set the threshold value as 60% of the maximum value for bone density. To leave thick and principal blood vessels, we set a threshold value for the flow rate of

the blood vessel—then vascular regression is limited by the flow rate.

4. Results and Discussion

The computational domain was a cube of 1 mm³ to eliminate the influence of boundaries. In our model, 90 particles were arranged in various directions; therefore, a total of 729,000 particles covered the entire area. The time step width was set to 0.1 steps/day. The total number of days for analysis was 90 days.

4.1 Analysis of Angiogenesis and Ca^{2+} Transport

The angiogenesis model and Ca^{2+} transport model, which influence bone regeneration, are analyzed in this section. As shown in Equation (1), diffusion of calcium corresponds to the rate of change in bone density. Therefore, the analysis results represent the distribution of calcium over time.

The calculation condition was as follows. In the initial state, five of the origin particles of angiogenesis are arranged in each of the XY planes. In other words, a total of 10 origin particles of angiogenesis are arranged in this analysis model. Blood vessels extend in the range from 0.01 to 0.13 mm once a day as time progresses. Then, they branch once, while blood vessels extend by 20 times. When a blood vessel reaches the opposite plane, extension ceases. When a blood vessel exceeds any of the four side planes by angiogenesis, the blood vessel is deflected onto the surface. Fig. 3 shows the analysis results of angiogenesis and Ca^{2+} transport. For convenience, the graph is color-coded according to the origin points of angiogenesis.

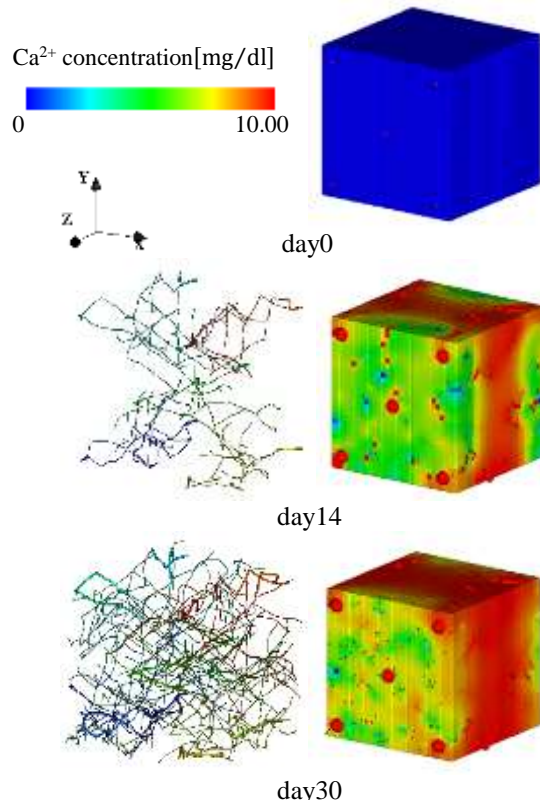


Fig. 3 Analysis of angiogenesis and Ca^{2+} transport

BME0005

The analysis results in Fig. 3 show that the blood vessels have grown from the origin points to cover the entire area while continuing to extend and branch. They have also maintained a suitable distance from each other without contact. In addition, Ca^{2+} has diffused to the area around the blood vessels and has further spread throughout the entire area. The blood vessels finished growing when they reached the opposite side of the point of origin. All blood vessels, including the new blood vessels formed from branching, reached the opposite side and then angiogenesis stopped completely; this is when an equilibrium state of angiogenesis was achieved. Ca^{2+} diffusion lasted for a while after reaching an equilibrium state of angiogenesis. Ca^{2+} was equilibrated when the Ca^{2+} concentration was 10.0 mg/dl over the entire region, which is the Ca^{2+} concentration in blood. The coefficient of Ca^{2+} is set to $1.0 \times 10^{-13} [\text{m}^2/\text{s}]$ [12].

4.2 Analysis of Trabecular Bone Formation

In this section, an overall coupled analysis considering angiogenesis and mechanical factors was performed for 90 days using Equation (8).

In the initial state, bone density is arranged at random in the range of $0 \leq \rho \leq 0.001 \text{ mg/mm}^3$ in the entire area, as shown in Fig. 4. This arrangement is regarded as a uniform field because each bone density value in the initial state is small throughout the region[13].

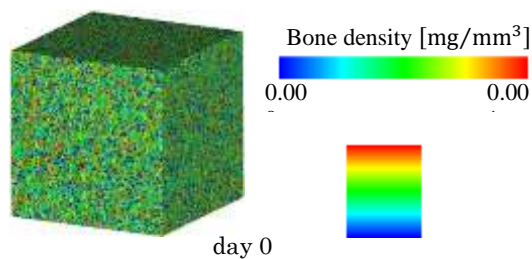


Fig.4. Initial bone density state

For the initial angiogenesis conditions, 5 origin particles of the blood vessels are arranged in each XY plane as described in section 4.1. Additionally, the enforced displacements of the same magnitude are given perpendicular to the respective boundary planes of the cube in the direction of compression, as in section 3.3.

Fig. 5 shows the analysis results of the coupled analysis of trabecular bone formation including angiogenesis and mechanical factors. The results 14, 30, and 90 day after surgery are shown. Red portions indicate the highest bone density, i.e., a state in which the bone is fully grown. Blue portions are hollow, where no bone is formed; they are called Volkmann canals. The results are influenced by both Ca^{2+} transport and mechanical stimulation.

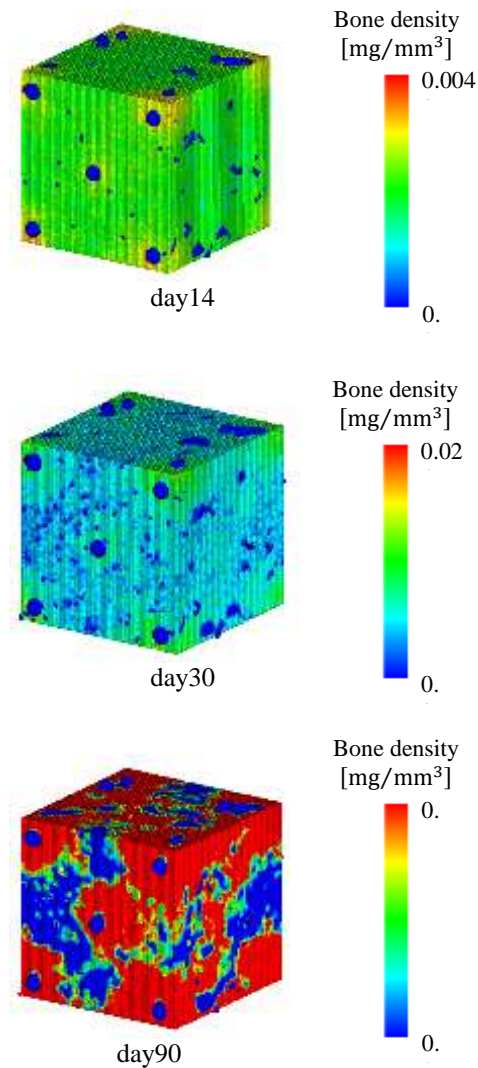


Fig. 5. The results of the coupled analysis of trabecular bone formation including angiogenesis and mechanical factors

In the results of Fig. 5, bone density increases over time, influenced by Ca^{2+} transport and mechanical stimulation. In addition, the bone structure is changed by the reaction-diffusion term. The bone structure on day 90 is similar to that in Fig. 2(c) compared with on day 30. These results indicate that the day by day bone remodeling progressed and the final bone structure has been successfully achieved. However, whether the bone structure is qualitatively right or not is yet to be verified.

4.3 Analysis of Vascular Regression

The flow of the vascular regression analysis is shown in section 3.6. Fig. 6 shows the result of that analysis. In the same way as section 4.1, the figure is color-coded according to the origin points of angiogenesis.

BME0005

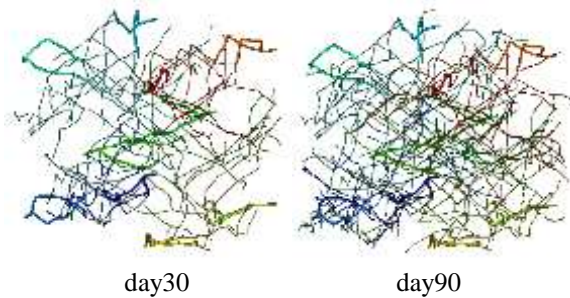


Fig. 6. Vascular regression analysis results

In the results shown in Fig. 6, the total number of blood vessels on day 90 is less than that on day 30. The tips of the thin blood vessels regressed, while major, large vessels have remained unchanged. Vascular regression takes place in conjunction with trabecular bone formation. Therefore, Fig. 6 is in agreement with the results presented in Fig. 5. This shows that thin blood vessels detect the bone density around them and regress by judging that it is no longer necessary to transport nutrition to those sites.

5. Conclusions

We built a model to predict the effects of angiogenesis and vascular regression on bone formation. Major factors of bone regeneration were modeled and analyzed in this study. In the angiogenesis model, blood vessels grew from the starting points and covered the entire area of the vessels. In the Ca^{2+} transport model, Ca^{2+} diffused into the area around the blood vessels and then spread throughout the entire area. In the trabecular bone formation analysis, which is affected not only by mechanical factors but also angiogenesis, we confirmed the differences in the strength and structure of the bone as the days passed. For blood vessels, angiogenesis occurred for up to 30 days to form a bone. After 30 days, the structural changes from immature bone to the trabecular bone progressed the regression of the blood vessels. We reproduced these phenomena during a 90-day-long experiment in this model.

In future, we expect to work on the elucidation of more detailed relations and mechanisms of bone formation and angiogenesis and regression to further improve the accuracy of the model. The model is expected to be applied in the area of tooth extraction analysis. In addition, patient-specific parameters such as homeostatic strain energy will be considered.

6. Acknowledgement

This work was supported by JSPS KAKENHI Grant Number 26420202.

7. References

[1]Masato, M., Okudera, T., & Iwamiya, M. (2011). Regeneration of microcirculation and alveolar bone after application of platelet-rich plasma. *Microvasular*

Reviews and Communications IV, 4: 12-17.

[2]Okudera, T., Masato, M., Iwamiya, M. (2010). Alveolar bone and microvascular changes after synthetic bone regeneration therapy using platelet-rich plasma. *Journal of Japanese Society of Oral Implantology*, 23: 18-25.

[3]Matsuo, M., Iwamiya, M., Saito, M., Todoki, K., & Kishi, Y. (2007). Regeneration processes of microcirculation of alveolar bone after synthetic bone graft using platelet-rich plasma (PRP). *Bulletin Kanagawa Dental College*, 35: 25-33.

[4]Okudera, T., Matsuo, M., & Iwamiya, M. (2010). Alveolar bone and microvascular changes after synthetic bone regeneration therapy using platelet-rich plasma (PRP). *Journal of Japanese Society of Oral Implantology*. 23: 18-25.

[5]Matsuo, M., Nakamura, T., Su, C., Shimomura, T., Kisara, K., Matsuda, D., Kishi, Y., & Takahashi K. (1998). Microvascular architecture of alveolar bone after guided bone regeneration with a resorbable membrane. *Japanese Journal of Oral Biology*. 40: 656-661.

[6]Tetsuya, T. (2010). *Biomechanics ~Fusion of mechanical engineering and biomedical~, OHM Co. LTD, Japan*

[7]Kozaburo, H. (2003). *Biomechanics of the remodeling of the living cells and tissues, CORONA PUBLISHING Co. LTD, Japan*

[8]Sakae, T. (2014). *Experimental medicine Bone metabolism Create, destroy and alter ~ The mechanism and the latest treatment ~, Yo-do Co. LTD, Japan*

[9]Ronald Ruimerman, *Modeling and remodeling in bone tissue: Technische Universiteit Eindhoven, 2005. Proefschrift. - ISBN 90-386-2856-0.*

[10]Carter, D. R., & Hayes, W. C. (1997). The compressive behavior of bone as a two-phase porous structure. *The Journal of Bone & Joint Surgery*. 59: 954-962.

[11]Yoshiki, H., Adachi, T., Tezuka, K., Tomita, Y. (2004). Computational simulation for trabecular regeneration in cancellous bone defect using a reaction-diffusion system model, *The Japan Society of Mechanical Engineers*. 04-40. 327-328.

[12] Hitomi, T., Takeda, N., & Iriya, K. (2009). Calculation of calcium diffusion coefficient of cement hardenings using minute pore data. *Obayashigumi gizyutsukennkyuusyohou (A house magazine of Obayasi Co. LTD)*.

[13] Kitamoto, A. and Nagayama, K. (2015). Numerical Simulation of Alveolar Bone Regeneration and Angiogenesis - Building a Coupled Model -, paper presented in The 6th TSME International Conference on Mechanical Engineering-BME 009, Hua-Hin, Thailand.